Ionic basis of the receptor potential in a vertebrate hair cell

D. P. Corey & A. J. Hudspeth

Division of Biology, California Institute of Technology, Pasadena, California 91125

Vertebrate hair cells, the primary receptors of auditory, vestibular and lateral-line organs, occur in epithelia which separate fluids of differing ionic composition. The apical surfaces of hair cells, on which the mechanosensitive hair bundles are situated, face a high-K^+ fluid (termed endolymph in the inner ear); the basolateral surfaces instead contact fluid (perilymph or a related substance) of a composition similar to that of other extracellular fluids[1-3]. The universal occurrence of high-K^+ fluid on the apical surfaces of hair cells in vertebrates has been taken as evidence that it is important for the transduction process, in particular that it relates to the ionic specificity[4] of the conductance change[5] underlying the receptor potential. There is, however, conflicting experimental evidence regarding this specificity. K^+ has generally been thought to carry the receptor current, as replacement of endolymph with perilymph in the guinea pig cochlea abolishes the extracellularly recorded microphonic potential[6]. Yet microphonic potentials, as well as intracellular receptor potentials, have been recorded in other preparations when the apical surfaces of the hair cells faced instead a high-Na^+ saline, and thus when the electrochemical gradient for K^+ was near zero[5,7]. Ca^{2+} has also been proposed to carry the receptor current[8], but its concentration is quite low in endolymph[3], particularly that of the mammalian cochlea[9]. We present evidence here that the receptor current in a vertebrate hair cell is carried *in vivo* by K^+, but that the transduction channel is in fact nonspecific, being permeable to Li^+, Na^+, K^+, Rb^+, Cs^+, Ca^{2+}, and at least one small organic cation.

Hair cells were prepared for intracellular recording as described previously[5,10]. Sacculi were removed from adult bullfrogs and their otolithic membranes peeled away after loosening by mild proteolysis (incubation for 60 min with 0.03 mg ml^{-1} subtilopeptidase A, EC 3.4.4.16, at 22 °C). The tissue was positioned in an experimental chamber with standard saline on all cell surfaces and viewed with Nomarski differential interference contrast optics. Individual hair cells were penetrated by two glass microelectrodes, each 100–150 MΩ in resistance, connected to a simple voltage clamp circuit. To stimulate each impaled cell, its hair bundle was deflected with a fine glass probe (0.2 μm tip diameter) inserted horizontally between the kinocilium and the rest of the hair bundle. Probes were moved by an electronically controlled, two-dimensional stimulator, over a distance of 1–2 μm, with a 10-Hz, triangle waveform.

We first measured the current–voltage relationship for unstimulated hair cells (Fig. 1). The input resistance measured with two electrodes was 200–300 MΩ at a holding potential of −60 mV. Because the resistance was higher (200–900 MΩ) if measured with one electrode and an active bridge circuit, much of the apparent membrane conductance at this potential resulted from penetration damage. At membrane potentials more positive than about −50 mV, however, the resistance dropped to 6–7 MΩ. This conductance increase was largely blocked by 1 mM 3,4-diaminopyridine[11], and is evidently a voltage-dependent K^+ conductance. Such outward or delayed rectification may explain the rather small receptor potentials seen in some hair cell preparations[12,13]: because of the change in slope conductance, a receptor current which generates a receptor potential of 20 mV in bullfrog hair cells at a resting potential of −60 mV produces only 0.5 mV at −40 mV. Figure 1 shows an additional conductance increase, an inward or anomalous rectification, at potentials below −100 mV. Such a rectification has been hypothesised to explain certain aspects of electrical behaviour of the mammalian cochlea[14], but has not previously been demonstrated for vertebrate hair cells.

The stimulus-associated current, or receptor current, was measured by presenting periodic mechanical stimuli of saturating amplitude while clamping to various potentials. The receptor current at the holding potential of −60 mV ranged from 45 to 205 pA with a mean of 98 pA (±37 pA, s.d., $n = 28$ cells) and with the larger values more representative of healthy cells. Variation in the measured current was caused both by decline in the viability of a cell during prolonged recording and by mechanical drift of the stimulus probe with respect to the responsive range of the hair bundle. The voltage dependence of the receptor current was consequently determined by comparing the receptor current at a test potential to the current at the holding potential immediately before and after the potential step. The receptor current at −60 mV was normalised to 100 pA for each cell, and the receptor current at each test potential then scaled by the same amount. An implicit assumption in this analysis is that the mechanical sensitivity is not also voltage-sensitive, for instance that the responsive range of the hair bundle does not shift as the cell is depolarised.

A representative series of clamp records is shown in Fig. 2*a*. The receptor current reverses its direction from inward to outward at a membrane potential between −9 and +11 mV. Figure 2*b* combines normalised data from 24 cells; a linear regression fit to these data indicates a reversal potential of −2 mV. This is not the equilibrium potential for Na^+, K^+, or Ca^{2+}, since a standard, 124-mM Na^+ saline solution[5] faced all cell surfaces during these experiments. It could, however, result from a stimulus-dependent conductance that is nonspecific—that has a limited ability to discriminate among cations.

We consequently tested several cations using an *in vitro* microphonic technique[15]. The macular epithelium of the sacculus was positioned across a hole between two chambers, so as to separate them ionically and electrically. The potential across

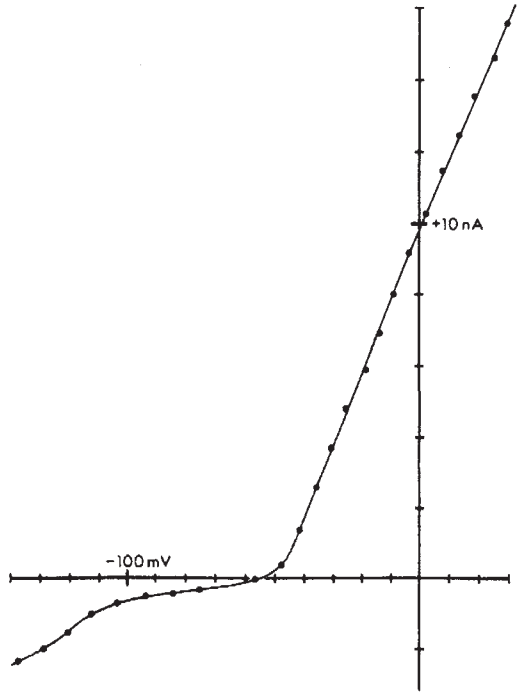

Fig. 1 Current-voltage relationship for a saccular hair cell, measured 50 ms after the start of a voltage step. Inward current is shown as negative. The holding potential was −60 mV. The striking outward rectification which occurs above −50 mV was blocked by 3,4-diaminopyridine and probably corresponds to the delayed rectification of most neurones. Inward or anomalous rectification is evident at potentials below −100 mV.

0028-0836/79/430675—03$01.00

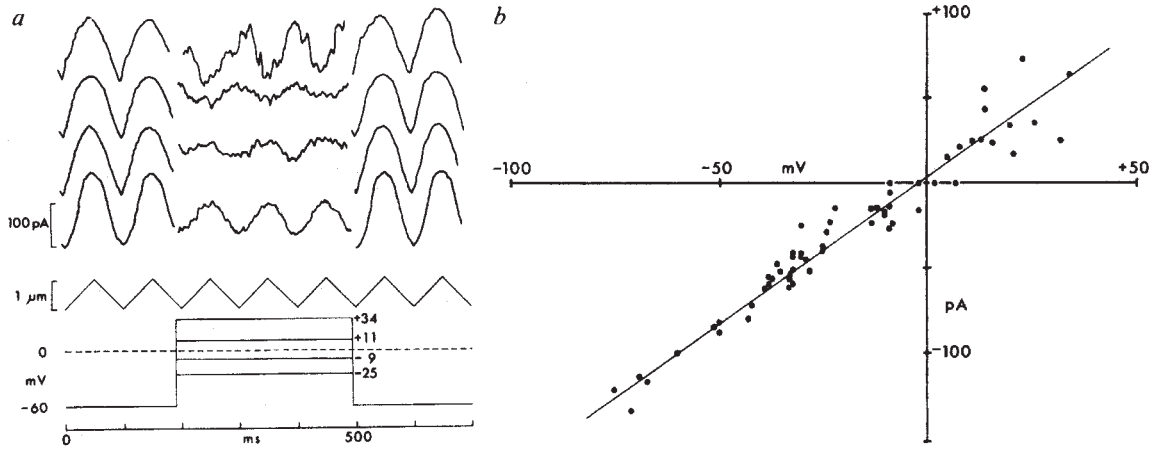

Fig. 2 *a*, Receptor currents at a holding potential of −60 mV and at test potentials of −25, −9, +11, and +34 mV; inward current is shown as negative. The membrane potential was held at −60 mV for 200 ms, clamped to the test potential for 300 ms, and returned to the holding potential. Each trace represents the average of 10 test steps. Ionic currents that were not stimulus-dependent were electronically subtracted before measuring the receptor current. The hair bundle was continuously moved with a 1.1-μm, 10-Hz, triangle-wave stimulus, shown below the current records; downward represents a deflection toward the kinocilium. *b*, Magnitude of the receptor current as a function of membrane potential; normalised data from 24 cells. The line is a linear regression fit to the data ($r^2 = 0.97$); its zero-current intercept, the reversal potential, is −2 mV. The external fluid was standard, high-Na^+ saline, so that the reversal potential is not the equilibrium potential of Na^+, K^+, or Ca^{2+}.

the epithelium was monitored with an electrode in each chamber; a second pair of electrodes was used to pass current to clamp the transepithelial potential at zero. Measuring the transepithelial current, rather than the transepithelial potential, avoided variations in response amplitude caused by slow changes in epithelial resistance. Hair cells were stimulated *en masse* by moving the otolithic membrane, which remained attached to the hair bundles, with a glass probe driven by a piezoelectric element. The stimulus was a saturating step displacement of amplitude 1.5 μm and duration 1 ms. The otolithic membrane can follow this fast stimulus, and the microphonic current turns on and off in much less than this time[15]. The charging time of the hair cell membrane is much longer, however, so that the intracellular potential should change only slightly during the pulse. The measured current is accordingly dependent on the resting potential and the permeability to the test ion, but not on voltage-sensitive conductances that are secondary to the receptor potential.

The chambers were separately perfused with a test solution on the apical side (130 mM of the relevant monovalent cation, 0.25 mM Ca^{2+}, 130 mM Cl^-, 3 mM D-glucose, 1 mM HEPES) and an artificial perilymph on the basolateral side (3.63 mM K^+, 122 mM Na^+, 1.36 mM Ca^{2+}, 0.68 mM Mg^{2+}, 130 mM Cl^-, 3 mM D-glucose, 1 mM HEPES). The apical surfaces of hair cells and supporting cells are bounded by tight junctions, which limit the exchange of ions between the two chambers.

All of the alkali cations supported the microphonic current. The mean relative signal amplitudes from eight experiments were: Li^+, 0.9; Na^+, 0.9; K^+, 1.0; Rb^+, 1.0; and Cs^+, 1.0. Ammonium ion (NH_4^+) was more permeant, with a relative amplitude of 1.3. To establish whether still larger ionic species could traverse the transduction channel, we bathed the apical surface with test solution containing 130 mM tetramethylammonium ion (TMA). This reduced the microphonic current to 0.2 of its value for 130 mM K^+, suggesting that TMA can pass through the transduction channel, although less readily than the alkali cations. To confirm this observation, TMA was tested on single cells using the intracellular voltage clamp method. The reversal potential, with 130 mM TMA on all cell surfaces, was −25 mV. Assuming that the extracellular TMA activity is roughly the same as the intracellular K^+ activity, this indicates a channel permeability to TMA about 0.4 that of K^+ (refs 16, 17). The fact that the permeabilities estimated by ionic current and by reversal potential are not equal suggests that TMA partially blocks the transduction channel[18].

The ability of one divalent ion, Ca^{2+}, to pass through the transduction channel was also demonstrated by extracellular recording. With 87 mM $CaCl_2$ in the test solution at the apical surface of the hair cell, the microphonic current was 0.3 that produced by 130 mM K^+. Because its concentration in endolymph is very low, Ca^{2+} can carry very little of the receptor current *in vivo*. Ca^{2+} does seem, however, to be a necessary cofactor for the response[5,8]: with a 130-mM K^+ saline, the microphonic current was abolished if the Ca^{2+} concentration was reduced below about 10 μM. Sr^{2+} replaces Ca^{2+} in this role, but Mg^{2+} and Ba^{2+} do not.

Because the transduction channel in frog saccular hair cells is nonspecific, the transduction current *in vivo* will be carried by cations approximately in proportion to their concentrations in endolymph. K^+, the predominant ion, will normally carry most of the current. The channel is equally permeable to the other alkali cations, however, and moderately permeable to Ca^{2+} and to an organic cation, TMA. As the unhydrated diameter of TMA is 0.54 nm, the channel interior must be at least this large. It therefore resembles the nonspecific, acetylcholine-activated channel of the motor endplate, which has an internal diameter of at least 0.65 nm (ref. 19).

It remains to be seen whether the transduction channels of all vertebrate hair cells are comparably nonspecific. The fact that Na^+ can support transduction in the goldfish sacculus[7] suggests that the channels in this organ are also nonspecific. The argument that ions other than K^+ cannot carry transduction current in the mammalian cochlea rests on the observation that substitution of Na^+ for K^+ in cochlear endolymph gradually but irreversibly blocks the response[6]. This might, however, reflect secondary effects of Na^+ accumulation on hair cells, such as the metabolic work required to pump this ion out of cells, rather than an inability of Na^+ to carry receptor current into cochlear hair cells. Inasmuch as the hair cells of lower vertebrates share with those of the cochlea a transduction process operating in high-K^+ fluid, mediated by stereocilia[10], and capable of great speed[15], it seems likely that the transduction channel of cochlear hair cells is also nonspecific in its ionic selectivity.

We thank Dr S. J. Krasne for helpful discussions, Mr J. H. R. Maunsell for assistance with data processing, and Mr R. Jacobs for technical assistance. This work was supported by NIH grants NS-13154 and GM-07616 and by the Ann Peppers and William Randolf Hearst Foundations.

Received 18 July; accepted 14 September 1979.

1. Smith, C. A., Lowry, O. H. & Wu, M. L. *Laryngoscope* **64**, 141–153 (1954).
2. Russell, I. J. & Sellick, P. M. *J. Physiol., Lond.* **257**, 245–255 (1976).
3. Peterson, S. K., Frishkopf, L. S., Lechène, C., Oman, C. M. & Weiss, T. F. *J. comp. Physiol.* **126**, 1–14 (1978).
4. Sellick, P. M. & Johnstone, B. M. *Prog. Neurobiol.* **5**, 337–362 (1975).
5. Hudspeth, A. J. & Corey, D. P. *Proc. natn. Acad. Sci. U.S.A.* **74**, 2407–2411 (1977).
6. Konishi, T., Kelsey, E. & Singleton, G. T. *Acta otolaryngol.* **62**, 393–404 (1966).
7. Matsuura, S., Ikeda, K. & Furukawa, T. *Jap. J. Physiol.* **21**, 563–578 (1971).
8. Sand, O. *J. comp. Physiol.* **102**, 27–42 (1975).
9. Bosher, S. K. & Warren, R. L. *Nature* **273**, 377–378 (1978).
10. Hudspeth, A. J. & Jacobs, R. *Proc. natn. Acad. Sci. U.S.A.* **76**, 1506–1509 (1979).
11. Kirsch, G. E. & Narahashi, T. *Biophys. J.* **22**, 507–512 (1978).
12. Harris, G. G., Frishkopf, L. S. & Flock, Å. *Science* **167**, 76–79 (1970).
13. Weiss, T. F., Mulroy, M. J. & Altmann, D. W. *J. acoust. Soc. Am.* **55**, 606–619 (1974).
14. Hubbard, A. E., Geisler, C. D. & Mountain, D. C. *J. acoust. Soc. Am.* **61**, Suppl. 1, S95 (1977).
15. Corey, D. P. & Hudspeth, A. J. *Biophys. J.* **26**, 499–506 (1979).
16. Goldman, D. E. *J. gen. Physiol.* **27**, 37–60 (1943).
17. Hodgkin, A. L. & Katz, B. *J. Physiol., Lond.* **108**, 37–77 (1949).
18. Hille, B. in *Lipid Bilayers and Biological Membranes: Dynamic Properties* (ed. Eisenman, G.) 255–323 (Dekker, New York, 1975).
19. Dwyer, T. M., Adams, D. J. & Hille, B. *Biophys. J.* **25**, 67a (1979).

Inhibition of platelet aggregation by native and desialised alpha-1 acid glycoprotein

Michael Costello, Barry A. Fiedel & Henry Gewurz

Department of Immunology, Rush University and Department of Microbiology and Immunology, University of Illinois at the Medical Center, Chicago Illinois 60612

The alpha-1 acid glycoprotein (orosomucoid; AAG) is a normal constituent of human plasma (650 ± 215 μg ml^{-1}) which increases in concentration as much as fivefold in association with acute inflammation and cancer, and thus is recognised as an acute phase protein[1,2]. AAG consists of a single polypeptide chain, has a molecular weight of 44,100, and contains ~45% carbohydrate including 12% sialic acid; it is the most negatively charged of the plasma proteins[3]. Certain of the biological properties of AAG are related to its sialic acid content[1,3]; thus, clearance and immunogenicity of AAG are markedly increased on desialisation[4,5]. The biological functions of AAG are largely unknown. AAG has the ability to inhibit certain lymphocyte reactivities including blastogenesis in response to concanavalin A, phytohaemagglutinin and allogeneic cells[6], and these inhibitory effects are enhanced in association with desialisation[7]. In view of these observations, a report that unphysiologically large (5–15 mg ml^{-1}) amounts of AAG inhibit the platelet aggregation induced by ADP and adrenaline[8], and evidence that a sialic acid-deficient species of AAG appears elevated in several chronic disease states[9,10], we compared the effects of AAG and its desialised counterpart (AAG-D) on platelet aggregation. We report that desialisation of AAG is associated with increased expression of activity inhibitory to the platelet aggregation otherwise observed on stimulation with ADP, collagen or thrombin.

AAG was isolated from human pleural fluids as described previously[6]. The purity of the four AAG preparations tested was established by SDS-polyacrylamide gel electrophoresis, immunoelectrophoresis and column chromatography on Sephadex G-75 and DEAE-cellulose. Desialisation was performed using *Vibrio cholerae* neuraminidase according to Schmid[11], with subsequent removal of the neuraminidase by reisolation of the AAG using DEAE-cellulose column chromatography; >75% loss of sialic acid[12] and 52% decrease of relative mobility on electrophoresis in polyacrylamide gels[13] were observed. Absence of residual neuraminidase activity in the AAG-D preparations was established by incubation with native AAG as the substrate using conditions optimal for enzyme activity; no neuraminidase activity was detected

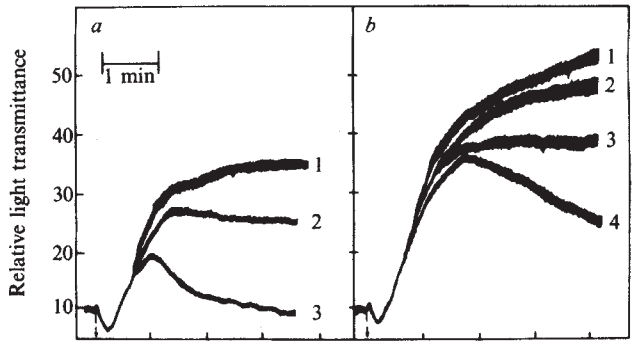

Fig. 1 Platelet aggregation induced by ADP at 12 μM (*a*) and 25 μM (*b*), and its inhibition by AAG and AAG-D. In *a*, curve 1 represents the buffer control; curve 2 inhibition by 2 mg ml^{-1} AAG; and curve 3 inhibition by 2 mg ml^{-1} AAG-D. In *b*, curve 1 represents the buffer control; curve 2 inhibition by 2 mg ml^{-1} AAG; curve 3 inhibition by 0.1 mg ml^{-1} AAG-D; and curve 4 the inhibition observed in the presence of 0.5–2.0 mg ml^{-1} AAG-D. AAG-D was substantially more inhibitory than the native molecule in all conditions tested.

(<0.017 units per mg AAG-D). The standard platelet reaction mixtures consisted of 500 μl platelet-rich plasma (PRP), 200 μl of a dilution of AAG or AAG-D (in phosphate-buffered saline) and various amounts (in 10–15 μl) of the aggregating agent; the platelets were preincubated with AAG or AAG-D in the aggregometer for 30 s before stimulation with ADP, acid-soluble collagen[14], or thrombin. In experiments involving platelet activation by thrombin, 500 μl of a washed platelet suspension (3.0×10^8 ml^{-1}) was used in place of PRP[15].

The addition of either AAG or AAG-D (2 mg ml^{-1}) to PRP resulted in inhibition of the platelet aggregation otherwise observed on challenge with 12 μm ADP (Fig. 1*a*). AAG-D was substantially more inhibitory than native AAG at all doses of the glycoprotein tested, with inhibition directly proportional to the concentration of AAG and AAG-D and inversely proportional to the intensity of the ADP challenge stimulus. Thus, on challenge with a larger amount (25 μM) of ADP, 2 mg ml^{-1} AAG was no longer inhibitory, while AAG-D remained inhibitory even at concentrations as low as 50 μg ml^{-1}; concentrations of AAG-D to 2 mg ml^{-1} did not induce substantially greater degrees of inhibition but did bring about deaggregation of the stimulated platelets (Fig, 1*b*). The inhibitory effects of AAG and AAG-D were directed preferentially against the secondary wave of platelet aggregation, although with low (4 μM) ADP stimulation a minimal inhibitory effect on the primary aggregation wave also was observed.

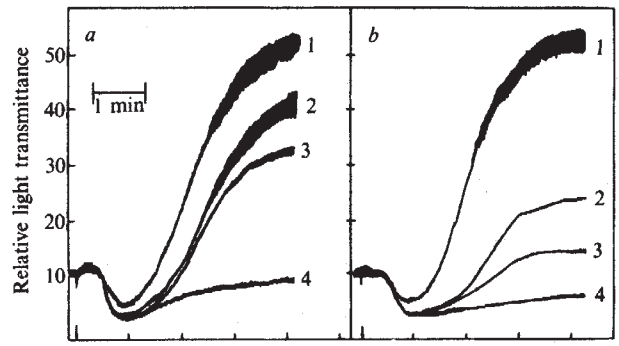

Fig. 2 Platelet aggregation induced by 9 μg ml^{-1} acid-soluble collagen and its inhibition by AAG (*a*) and AAG-D (*b*). In *a*, curve 1 represents the buffer control, while curves 2, 3 and 4 represent stimulation in the presence of 0.05, 0.5 and 2.0 mg ml^{-1} AAG, respectively. In *b*, curve 1 represents the buffer control, and curves 2, 3 and 4 show stimulation in the presence of 0.05, 0.1 and 0.5 mg ml^{-1} AAG-D, respectively. AAG-D again was substantially more inhibitory than the native molecule.

0028–0836/79/430677—02$01.00